ELSEVIER

Biochimica et Biophysica Acta 1231 (1995) 197–212

BBA Biochimica et Biophysica Acta

# Photoacoustic diagnostics of laser-induced processes in reaction centers of *Rhodobacter sphaeroides*

Oleg V. Puchenkov [1], Zohar Kopf, Shmuel Malkin *

*The Weizmann Institute of Science, Biochemistry Department, 76100, Rehovot, Israel*

Received 10 January 1995; accepted 27 April 1995

**Abstract**

A theoretical model of photoacoustic signal generation in a suspension of bacterial reaction centers (RCs) is suggested. The existing technique of separation of the two contributions to photoinduced volume changes (thermal expansion and structural rearrangement), based on their different temperature dependence, is extended to take into account the fact that they may also have different time dependence. In the practical implementation of the technique, it was found that electron transfer in the RC isolated from *Rhodobacter sphaeroides* is associated with a fast ( $< 100$ ns) contraction, $32 \pm 1$ Å$^3$, which has the same value within the accuracy of our measurements for wild-type and R-26 preparations. The enthalpy of the $P^+Q_A^-$ state deduced from our measurements is $0.56 \pm 0.04$ eV. The quantum yield of photochemistry, $\phi$, was measured in a broad range of background light intensities. Its value for dark-adapted RCs, $\phi \approx 1.0$, decreased continuously to $\phi \approx 0.3$ at background light intensity $\approx 1$ photon/(RC · s). Reduced values of $\phi$ observed after long background light illumination were attributed to reversible structural changes, which relax in about 15–20 min after charge recombination. In the photochemically 'closed' reaction center, a deactivation process, following laser excitation, involves a long-lived intermediate state characterized by an exponential decay with a lifetime of $620 \pm 80$ ns and an amplitude of $0.14 \pm 0.04$.

*Keywords:* Photoacoustic diagnostics; Photoinduced volume change; Reaction center; Relaxation kinetics; Nonlinear optimization; (*R. sphaeroides*)

## 1. Introduction

The kinetics of electron transfer reaction in photosynthetic bacterial reaction centers (RCs) is usually monitored by ultrafast transient absorption spectroscopy [1], revealing intermediate states formed during the electron transfer. Possible contributions of various RC conformers and unrelaxed states to the spectral and kinetic data [2] prompted experiments aimed at identifying photoinduced structural changes in pigment/protein complex [3–5]. Valuable direct information about the dynamics of the structural changes may be obtained by laser-induced photoacoustic (PA) measurements [6]. The PA technique enables the determination of volume changes during photoinduced reactions and discrimination between that part of the excitation energy which is released as heat and the part stored in long-lived intermediate species [7].

The PA method was used previously to study photochemical processes in RCs on the millisecond [8,9] and microsecond [10] time scales. It was found that the photochemical event is accompanied by a negative volume change (contraction), attributed, by comparison with other kinetic information, to the electron transfer between the primary donor (bacteriochlorophyll dimer) and the primary quinone acceptor. This contraction should be taken into account to obtain a correct value of the photochemical energy storage [10]. Proper interpretation of the volume changes following the laser flash requires a method of separation of the two possible contributions: the thermal expansion and the contraction due to the structural rearrangement. The separation could be based upon a different dependence of the two contributions on varying experimental conditions. Two approaches were suggested [8,11]. The approach proposed in [8] makes use of the fact that only the thermal expansion part depends substantially upon the solution temperature, so one can identify the two contributions by varying the temperature. This procedure is particularly suitable for investigation of aqueous solutions, where at $\sim 4$°C only photochemical volume changes can

* Corresponding author. Fax: +972 8 344118.

[1] Permanent address: N.N. Andreev Acoustics Institute, Moscow, Russia.


*SSDI* 0005-2728(95)00078-X

be observed, since at this temperature the thermal expansion coefficient of water is zero. Another possibility is to use a two-component mixture as a solvent and to change the thermophysical parameters of the solution, affecting the PA signal generation, by alteration of volume fractions of the components in the mixture [11]. The latter method, however, turned out to be less sensitive to small photochemical volume changes, and cannot be used to interpret the PA data obtained on the photoactive system with unknown kinetics of structural changes and heat release.

Although the shapes of transient PA signals were recorded previously with submicrosecond time resolution, only the amplitude (or peak-to-peak value) of the PA signal was in effect used for the calculations [10,11]. Thus, in the previous work [10], the peak-to-peak value was chosen as a parameter for determination of the saturation profile of the molecular volume changes as a function of absorbed laser energy $\Delta V_p(E)$. The initial slope of this dependence divided by the ratio of the saturation value, $\Delta V_p|_{E\to\infty}$, to the number of reaction centers exposed to the light gives the photochemical quantum yield. However, this procedure is inherently imprecise. The first problem is to determine the saturation value which could not be reached, and, therefore, should be found by an arbitrary extrapolation. The second problem lies in the estimation of the number of RCs exposed to the light for a non-uniform laser beam. Moreover, the time dependencies of the heat release and the photochemical volume changes may be different, thereby leading to different shapes of PA signals for the two contributions and complex evolution of the net PA signal, as will be shown here. Therefore, a more accurate, dynamic approach to the separation is needed, which, by definition, deals with the entire time profile rather than with the amplitudes [12]. Careful examination of the PA waveforms is necessary to reveal the kinetics of the volume changes in order to assign them to a particular step of the electron transfer.

In this work we follow the general methodology for PA experiments detailed in [13]. Dynamic analysis of the PA signal, combined in a suspension of photosynthetic RCs from the thermal and molecular volume change contributions, is made in a wide range of laser energies. Interpretation of the observed photoinduced volume variations as an evidence of a conformational change that occurs during the electron transfer reaction makes the PA measurements a sensitive tool to probe photochemical activity [14]. We used the detection of the photoinduced contraction to estimate the quantum efficiency of photochemistry under varying experimental conditions, and examined the saturation of the photochemical activity by an actinic light illumination.

## 2. Materials and methods

*Rhodobacter sphaeroides* carotenoidless mutant R-26 and wild-type reaction centers (RCs) were prepared as reported [10] and kept frozen at −20°C until use. Preparations contained two quinones per RC, that was checked by procedure described in [15]. Batch preparation and dilution

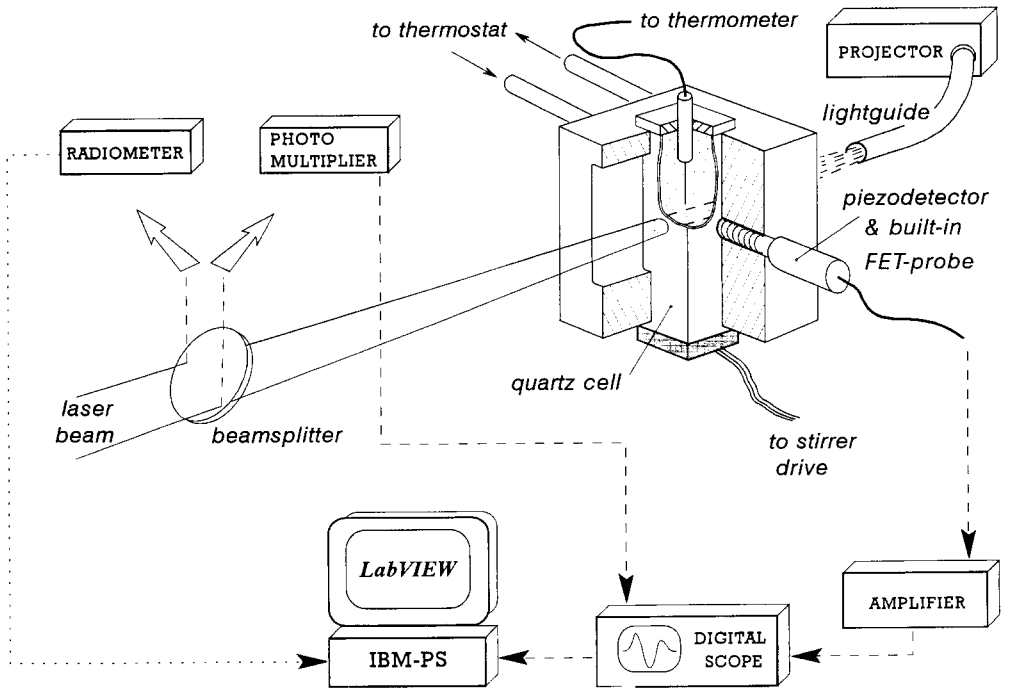


Fig. 1. Scheme of the PA experiment.

was carried out in a TL buffer (Tris 10 mM, EDTA 1 mM, LDAO 0.1% (pH 8), double-distilled water). The solutions prepared were introduced into standard measuring spectroscopic cells (optical path 1 cm) through a 1 $\mu$m size filter (Millipore) to eliminate microparticles which could induce scattering of the laser pulse and thereby cause spurious acoustic response. The absorption spectra of the samples were measured in the range 250–900 nm on a Spectronic 1201 spectrophotometer (Milton Roy) just before and 10–15 min after the PA experiment.

The set-up of the PA experiment was similar to that used in [10], with modifications (Fig. 1). For excitation, the second harmonics of a mode-locked Nd:YAG laser (Quantel YG571) was used (pulse duration $\tau \approx 35$ ps, wavelength $\lambda \approx 532$ nm). The cell was tightly fixed in a brass holder to provide a good thermal contact. The holder had a cavity for pumping a cooling agent (1/1 mixture of water and ethylene glycol) from a thermostat (Neslab RTE-110). The surface of the holder was thermally insulated with a porous rubber to prevent accumulation of moisture at low temperatures on the cell walls facing the laser beam. For the same purpose, the front and back walls of the cell were flushed with dry nitrogen. This design does not provide a uniform cooling, so that temperatures near the front and back cell walls are higher than in the center of the cell. Therefore, it was important to monitor the temperature precisely in the center of the cell where the laser-induced PA signal originates. For this we used a needle-like probe of T-type thermocouple thermometer (Sensortek BAT-10), positioned very close to the laser light pathway (see the sketch in Fig. 1). The temperature was monitored with an accuracy $\pm 0.1$°C and the variations of the sample temperature during PA experiment due to thermal convection were within $\pm 0.2$°C. Experiments were carried out in the temperature range 1–28°C. To equalize the temperature inside the cell and to refresh the portion of the sample exposed to the laser beam, the content of the cell was periodically stirred with tiny magnetic bar driven by mini-magnetic-stirrer (Hellma, CUV-O-STIR 333).

The pressure detector consisted of a ceramic PZT disk (diameter 4.7 mm, thickness 2.8 mm, Vernitron) enclosed in a stainless steel housing and loaded on a FET-probe preamplifier. The maximum spectral sensitivity of the detector found in a calibration experiment was equal to 0.47 mV/Pa. The detector was pressed against the side wall of the cell as shown in Fig. 1 with a small amount of vacuum grease for acoustic coupling. The signal from the detector was amplified 500–1000-times (Ithaco 1201 low noise preamplifier), recorded by digital oscilloscope (LeCroy 3910) and sent through a GPIB interface to a PS/ValuePoint-486/66 computer for further processing. PA waveforms were detected as an average of 50–70 signals with a repetition rate of 1 Hz.

The laser beam inside the cell, after optical conditioning with a system of lenses and a pinhole, was nearly parallel, with a Gaussian cross-sectional distribution. The distribution was directly measured by a moving knife-edge technique. The effective radius of the distribution, $a = 0.6$ mm, was chosen to match the transfer function of the detection system (the optimization of PA measurements is discussed in detail in [13]). The energy of the laser light

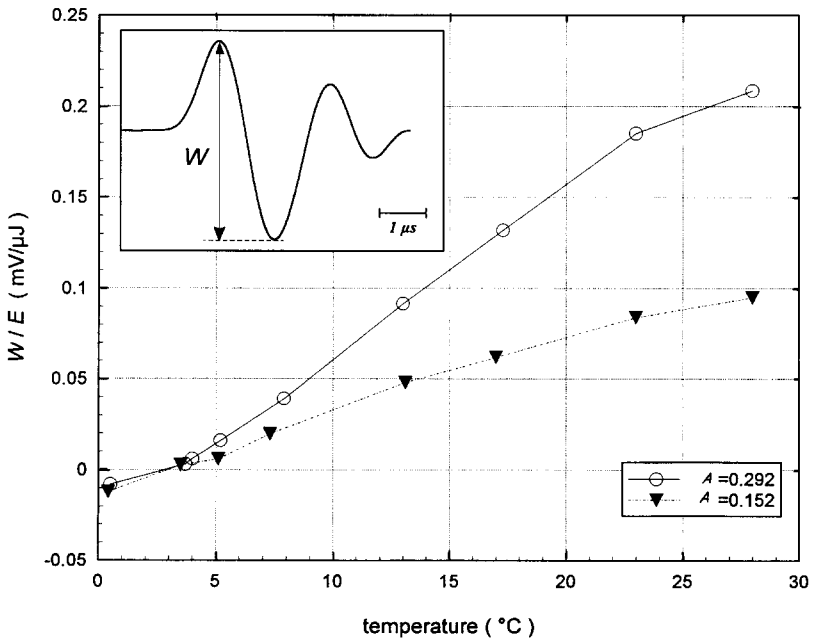


Fig. 2. Temperature dependence of the PA signal peak-to-peak value measured in $CoCl_2$ TL buffer solution. In the inset the shape of the PA signal measured in the reference solution at $T = 25$°C is shown.

was adjusted by means of neutral density filters, and measured with a pyroelectric radiometer (Laser Probe Inc. Rm-3700 with RJP-735 probe). In a number of experiments the cell was irradiated by continuous actinic light from Volpi Intralux 5000 projector. The spectral content of this light was adjusted by a long-pass colored glass filter (Schott RG-655), and the beam was directed in the region of the laser light absorption in the cell by means of a light guide. The results of the laser energy measurements for each shot were transferred to the computer through an RS232 interface, and stored with a corresponding PA waveform for further processing. Reliable timing of data acquisition was provided by a subnanosecond rise-time triggering signal from an ultrafast phototube (Hamamatsu R1193U-01). Data acquisition, on-line monitoring, and PA signal processing were done under control of virtual instrument written on LabView 3.0 software (National Instruments).

The PA experiment started with a calibration aimed at determining the dependence of measured PA signals on the sample temperature $T$, the absorbance of the sample at the laser wavelength $A_\lambda$, and the laser beam energy $E$. For this calibration, $CoCl_2$ (Fluka) solutions were used as calorimetric references, using the assumption that the thermoelastic properties of the TL buffer solutions of $CoCl_2$ are identical to those of RCs solutions [10]. The PA signal in the calorimetric reference does not change its shape with a variation of $E$, and $A_\lambda$ (in the range $A_\lambda \sim 0.1-0.3$). This shape was recorded at $T = 25°C$ (inset in Fig. 2), where the signal-to-noise ratio was $> 300$. With the decrease of the temperature, the polarity, but not the shape, of the signal is changed during the transition from $T > 4°C$ to $T < 4°C$ (some deviations from the shape shown in Fig. 2 are observed only in the vicinity of the transition point, see below). Then, for the calibration it was enough to measure the peak-to-peak value of the signal, $W$, as a function of $T$, $E$ and $A_\lambda$. It was found, that $W$ has an exact linear dependence on $E$ in the total available energy range 0–300 $\mu$J. Therefore, the calibration data may be conveniently presented in the form $W/E = f(T, A_\lambda)$. The shape of this function for two $A_\lambda$ values in the range of our measurements $A_{532} = 0.1-0.3$ is shown in Fig. 2. In general, the temperature dependence of the PA signal amplitude in water solutions is mainly determined by the strong dependence of their expansion coefficient, $\beta$. In distilled water, $\beta$ changes its sign at $T = 3.98°C$ [16], and in low concentrated aqueous solutions at slightly shifted temperatures. Nevertheless, some residual PA signal exists even at this transition temperature (possible reasons are discussed in [12,17]), which in our case is well above the noise level of our detection system (Fig. 3). Because complex residual waveform does not have unambiguous peak-to-peak value, the 'zero thermal contribution' temperature was taken as a point where the energy of the signal observed is minimal. For the TL buffer, it is 3.5°C. The experimental noise was estimated from measurements in pure double distilled water ($A_{532} \sim 5 \cdot 10^{-4}$ [18]), where the true signal is insignificant. The noise level was found to be independent of the laser energy in the range 0–100 $\mu$J; hence, the scattering of the laser beam on the cell walls is negligible.

The minimum residual PA signal in the TL buffer

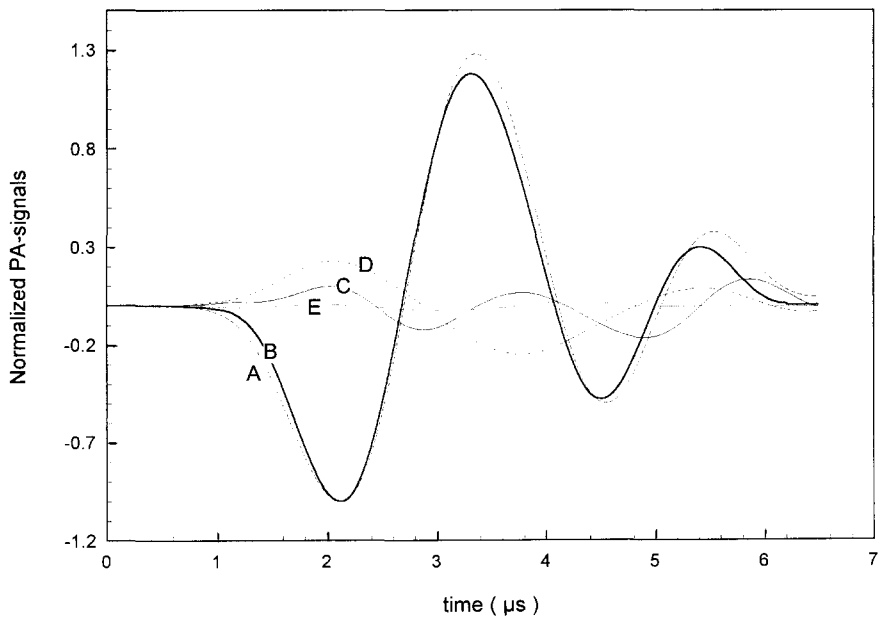


Fig. 3. Normalized PA signals observed at 3.5°C in suspension of RCs (A) at $E = 314$ $\mu$J (11.1 ph/RC), (B) at $E = 4.2$ $\mu$J (0.15 ph/RC); (C) at $E = 90$ $\mu$J (3.1 ph/RC) in a sample saturated by white actinic light of intensity $> 10$ ph/RC (internal reference); (D) in the reference solution at $E = 45$ $\mu$J, and (E) in double distilled water at $E = 40$ $\mu$J. Normalization constants used: A, 5.54 mV; B, 0.43 mV; C, 0.53 mV; D, 0.52 mV; E, 0.55 mV.

solution of $CoCl_2$, which was observed at $T \approx 3.5$°C may be considered as a small background for the measurements in RCs suspension, where the PA signal is generated by photoinduced contraction (PIC) of non-thermal origin. The shapes of the signals observed at 3.5°C both in the reference, and in the RCs suspension are shown in Fig. 3 in comparison with a spurious signal measured in distilled water at $T = 28$°C. Along with external reference ($CoCl_2$ solutions) we did the measurements with internal reference, i.e., on the sample solution where photochemistry is heavily saturated by strong (> 10 photons/RC) actinic light illumination [19], so no appreciable photochemical volume changes are expected. The minimal residual signal in internal reference is also observed at 3.5°C, and is about ~ 1% of the corresponding signal measured without illumination (note the energies and normalization constants listed in the caption of Fig. 3). The normalization constants for the waveforms in Fig. 3 are chosen in such a way as to show clearly the difference between the shapes of the PIC contributions for low and high laser energies.

At temperatures above 3.5°C the PA signal is combined from PIC and thermal expansion (THE) contributions. They have opposite signs and different dependencies upon the temperature and the laser energy [10]. Provided the two contributions have the same temporal profile, it could be expected that for some particular combination of $T$ and $E$ they will cancel each other. However, in our experiments we found that the combined PA signal never became zero. A typical transformation of the PA waveform at $T > 3.5$°C as the laser energy increases is shown in Fig. 4 for $T = 25$°C. At low energies the signal is dominated by the PIC contribution whereas at high energies the thermal expansion is superior. At intermediate energies complex PA waveforms are observed. They are not similar, either to the THE or to the PIC contribution, so these two contributions have different shapes. One cannot therefore use solely the amplitudes of PA signals, as this may lead to mistakes in the estimation of the two contributions, and hence in the resulting evaluation of the energy storage. In addition, for proper substraction of the PIC contribution measured at 3.5°C from the total PA signal measured at the room temperature an accurate correction of the time arrival of the PIC contribution is required. The arrival time varies because of the temperature dependence of the speed of sound (e.g., at room temperatures $\partial c/\partial T \approx 3$ m/s per C° [20]), slight misalignment of the laser beam axis from one measurement to another and also due to jittering of the triggering pulse. Therefore, the experimental accuracy may not be sufficient for the proper separation of the two contributions by a simple substraction. For a suitable interpretation of the PA signals a procedure of dynamic separation of the two contribution is needed, which should be based on a theoretical description of the waveforms generated in the RCs suspension. This description is given in the next section.

### 2.1. Methodology of time-resolved PA measurements in photosynthetic samples

PA measurements of laser-induced photochemical processes in solution were carried out in many experiments (see [21] for a comprehensive review). The dynamics of a relaxation process with a known kinetics may be found by iterative approximation of the experimental waveforms with a synthetic waveform obtained by the convolution of a model relaxation function with the reference signal [22].

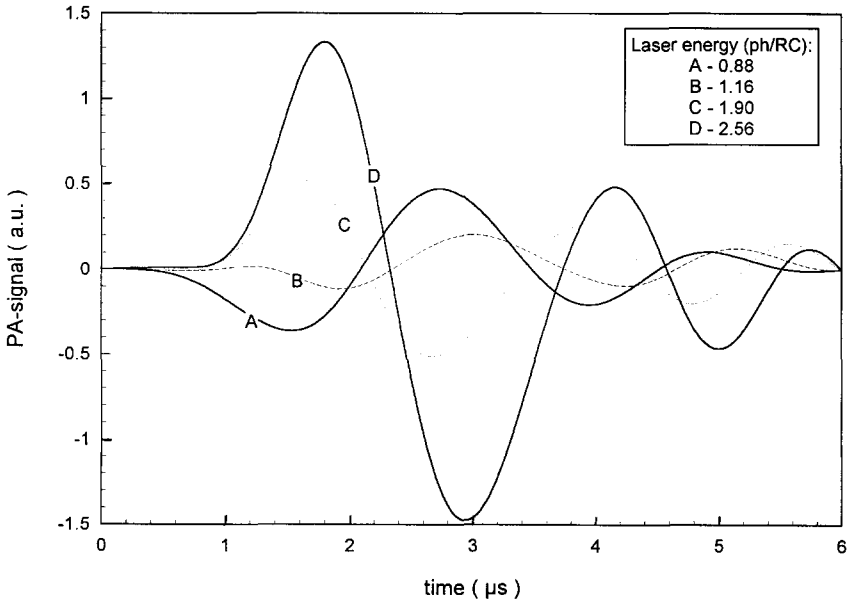


Fig. 4. Transformation of the PA signal shape with increasing laser energy.

However, an interpretation of the PA signals measured in RCs suspension is a more difficult task. First, the dynamics of thermalization of the absorbed energy in RCs is not known exactly; second, there is no information about the dynamics of protein conformational changes associated with the electron transfer reaction. Therefore, a general theoretical model for the interpretation of the PA signals should be developed.

The acoustic signal induced in a liquid by the absorption of laser pulse is described by a nonhomogeneous wave equation [12]. Solution of this equation can be conveniently presented in the frequency ($\omega$) domain. Taking into account the existence of conformational volume changes in photosynthetic samples [4–6], one has to write a general expression for the Fourier spectrum $U(\omega)$ of the electric signal in the output of the pressure detector as:

$$U(\omega) = \Gamma(\omega) K(\omega) [V_T(\omega) + V_P(\omega)], \quad (1)$$

where $V_T(\omega)$, $V_P(\omega)$ are Fourier spectra of relative volume changes associated with the thermal expansion and the molecular volume changes, respectively; $K(\omega)$ is the medium transfer function which describes the conversion of volume changes to the pressure signal and its subsequent propagation to the detector; $\Gamma(\omega)$ is the detector transfer function describing the process of pressure to voltage conversion.

In general, photoinduced volume changes of different origin are described by different functions of $\omega$, so that $V_T(\omega) \neq \text{const} \cdot V_P(\omega)$. Therefore, one of the primary goals of the calibration experiment is to find the combined transfer function, $\Gamma(\omega) \cdot K(\omega)$, which does not depend on the nature of the volume changes. Then, this function should be used for a suitable deconvolution analysis of the net PA signal.

Analytical expressions for the functions $K(\omega)$ and $\Gamma(\omega)$ for different geometries of the PA conversion and various types of thickness mode piezodetectors are given in [13]. For the cylindrical scheme of the PA conversion, considered here, the functions $K(\omega)$ and $V_T(\omega)$ for a reference solution have the form:

$$K(\omega) = \rho \frac{\pi}{2} \omega H_0^{(2)}(kl), \quad (2a)$$

$$V_T(\omega) = \frac{\mu\beta}{\rho C_p} \frac{E}{S} D(k) F(\omega), \quad (2b)$$

where $\rho$ and $C_p$ are, respectively, the density of the liquid medium and its heat capacity at constant pressure; $\mu$ is the light absorption coefficient; $\beta$ is the volume thermal expansion coefficient; $E$ is the total laser energy; $H_0^{(2)}$ is the Hankel function of the second kind; $l$ is the distance from the laser beam axis to the observation point; $k = \omega/c$ is the wavenumber of sound waves and $c$, the speed of sound; $D(k)$ is the Hankel transform of cross-sectional distribution of the laser beam $w(x,y)$ ($x$ and $y$ are the coordinates in the plane of the beam cross-section), which for a cylindrically symmetrical gaussian distribution used in our experiments is equal to $a^2/2\exp[-(ka/2)^2]$; $S$ is a normalization constant $S = \int\int w(x,y)\mathrm{d}x\,\mathrm{d}y$; $F(\omega)$ is the Fourier transform of a normalized time dependence $f(t)$ of the laser pulse intensity $I(t) = (E/S)f(t)$.

One important conclusion follows from analysis of expression (2): in the case of cylindrical geometry of the PA experiment the shape of the PA signal is determined not only by the dynamics of laser-induced volume changes but also by the shape of cross-sectional distribution of the laser intensity.

The general scheme of a PA experiment in suspension of RCs may now be outlined as follows. From the calibration experiment in the reference solution, where $V_P = 0$, and from the expressions for $V_T(\omega)$ and $K(\omega)$ given by Eqs. (2a,b), one can find the function $\Gamma(\omega)$ and the temperature dependence of thermoelastic coefficients for the sample solution. It is assumed that this dependence is mainly determined by the solvent (TL buffer) properties, and thereby will be the same for the reference and the sample solutions [10]. The cross-sectional distribution $w(x,y)$ should be also measured, and the corresponding function $D(k)$ should be calculated. In a second stage, from an experiment at 3.5°C (where $V_T = 0$) one can find the function $V_P(\omega)$ and measure the photochemical contraction. Finally, the PIC contribution, which supposedly does not vary with temperature [4], must be subtracted from the combined PA signal, measured at any other temperature, and the function $V_T(\omega)$ should be found.

Implementation of the procedure outlined requires no prior theoretical model of the energy deactivation and non-thermal volume changes. However, due to the nonlinear dependence of the PIC contribution on the laser energy (see [10]), the cross-sectional distribution of the volume changes does not follow the distribution of the laser light intensity $w(x,y)$. Therefore, the actual dynamics of the volume changes cannot be easily extracted from the $V_P(\omega)$ function. In addition, as was discussed above, the separation of the two contributions by a simple substraction of the PIC contribution measured at 3.5°C from the total PA signal measured at room temperature may not be sufficiently accurate.

Another way of the separation is suggested here. In the first step, taking into account preliminary results obtained in [10], one can develop a theoretical model for the PIC signal. The model should properly describe the non-linear dependence of the PIC signal on the laser energy, and also the observed changes in the signal profile with the increase of laser energy. Then, the model can be generalized to explain the time shift of the THE contribution at room temperature and the transformation of the combined waveforms (Fig. 4). The parameters of this model can be found by fitting experimental waveforms with two calculated functions $V_P(\omega)$ and $V_T(\omega)$. The goodness of the fit can be used to verify the consistency of the model.

*2.2. Theoretical model of photoinduced volume changes in suspension of RC for the cylindrical geometry of the PA experiment*

To obtain the dependence of the photoinduced volume changes on the laser pulse energy, we first consider the contribution of a small element of irradiated volume, where the energy absorbed is uniformly distributed. In the assumption that there is no excitation energy exchange between RCs, the number of photochemical events $Y$ may be calculated from the number of RCs, $L$, and the number of photons absorbed $M$ as in [23]:

$$Y = L[1 - \exp(-\phi M/L)] \quad (3)$$

where $\phi$ is the quantum yield of photochemical conversion of the absorbed photon energy. By attributing the values $Y, L, M$ per unit area across the laser beam, we can write for cross-sectional distribution of the photochemical events:

$$Y(d) = L\left[1 - \exp\left\{-\phi\frac{(E_a/e_\lambda)(w(d)/S)}{L}\right\}\right] \quad (4)$$

where $E_a$ is the absorbed laser energy; $e_\lambda$ is the energy of a photon at the laser wavelength; $d$ is the distance from the laser beam axis (we assume axial symmetry of the distribution: $w(x,y) = w(d)$). The concentration of RCs may be found from the measurements of the absorbance at some specific wavelength. We chose for this purpose the wavelength 802 nm near the maximum of absorption. Then, taking into account the value of molar extinction coefficient for this wavelength $\epsilon_{802} = 288 \pm 14$ $mM^{-1}$ $cm^{-1}$ [24], one can calculate $L = N_a A_{802}/\epsilon_{802}$ (where $N_a$ is the Avogadro's number).

The fact that the PIC signal was not observed in quinone-depleted RCs [10] enables the photoinduced contraction to be considered as being directly associated with the primary stable electron transfer reaction. Assuming that each photochemical event contributes a particular volume change $\nu_0$ into the net observed photochemical contraction $V_P$, the rate of the changes may be written as $\partial V_P/\partial t = \nu_0 \partial L'/\partial t = \nu_0 g(t)$ (where $L'$ is the number of photochemically transformed RCs, and the normalization condition applied: $\int g(t)dt = 1$). Then, the term for volume changes in (1) may be written in the form:

$$V_P(\omega) = \frac{\nu_0}{l} LG(\omega)\mathrm{II}\left\{1 - \exp\left(-\phi\frac{(E_a/e_\lambda)(w(d)/S)}{L}\right)\right\}, \quad (5)$$

where $l$ is the path of the laser beam in the cell; $G(\omega)$ is the Fourier transform of $g(t)$; and II{..} denotes the Hankel transformation. As can be seen from Eq. (5), even for instantaneous changes (i.e., $G(\omega) = 1$) the spectrum $V_P(\omega)$ will differ from the spectrum $V_T(\omega)$ measured in the reference solution (note that picosecond laser pulse used in our experiment gives rise to $F(\omega) = 1$). The two spectra are identical only in the limit of $E_a \to 0$, but they are increasingly different at high laser energies.

The number of photochemical events given by Eq. (3)

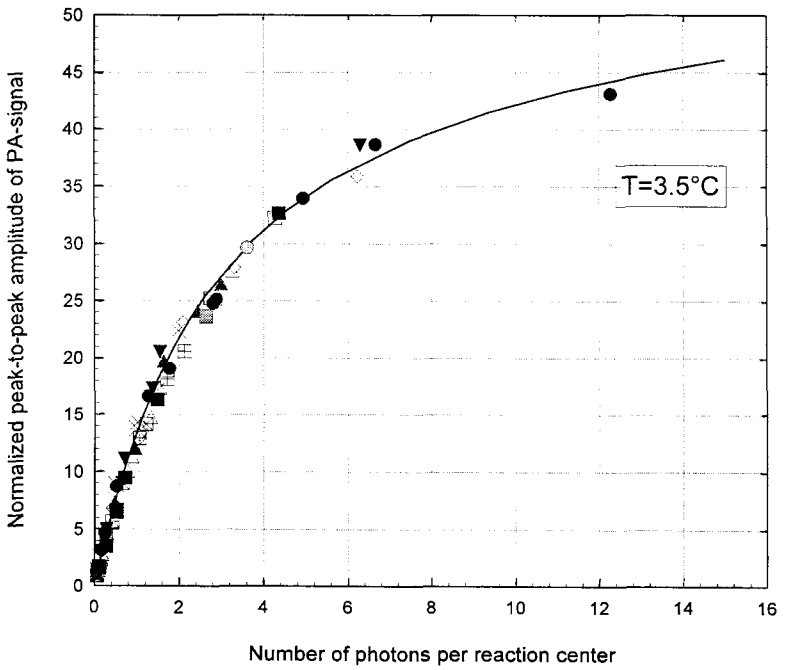


Fig. 5. Energy dependence of peak-to-peak amplitude of the PA signal normalized on the number of RCs. Theoretical curve calculated from Eq. (5) with parameters $\nu_0 = 32$ Å$^3$ and $\phi = 1$.

may be also considered as the number of photons which induce the photochemical reaction. The energy of these photons is partially dissipated as a heat, and partially stored as the energy of intermediate species. The balance between these two parts is altered with time following the different steps of the electron transfer. The chain of reactions $P^*IQ_AQ_B \rightarrow P^+IQ_A^-Q_B$ in RCs takes approximately ~ 200 ps [25]. This time is far beyond the resolution of PA measurements. The step $P^+IQ_A^-Q_B \rightarrow P^+IQ_AQ_B^-$ takes approx. 100 $\mu$s and is too slow to be resolved [13]. Therefore, the energy of the long-lived $P^+IQ_A^-Q_B$ state may be considered as an energy storage from the viewpoint of PA measurements, because this energy does not contribute to the PA signal. Let us designate the stored fraction of the photon energy as $\alpha$. Then, the part of this energy released promptly (on the time scale of the PA experiment) as heat is $(1-\alpha)e_\lambda$.

In addition to 'photochemical' photons there are also other absorbed photons which do not produce any stable photochemistry. The dynamics of the thermalization of their energy may be generally described by some relaxation function $r(t)$ (with a corresponding relaxation spectrum $R(\omega)$). According to this model, the part of volume changes produced by the thermal expansion may be written in the form:

$$V_T(\omega) = \frac{\mu\beta}{\rho C_p} E\left[\left(\frac{D(k)}{S} - \frac{e_\lambda L}{E_a}\mathrm{II}\left\{1-\exp\left(-\phi\frac{(E_a/e_\lambda)w(d)/S}{L}\right)\right\}\right)R(\omega) + (1-\alpha)\frac{e_\lambda L}{E_a}\mathrm{II}\left\{1-\exp\left(-\phi\frac{(E_a/e_\lambda)w(d)/S}{L}\right)\right\}\right], \quad (6)$$

The model suggested comprises three parameters $v_0$, $\phi$ and $\alpha$, and two relaxation functions $g(t)$ and $r(t)$, that should be found from PA experiment. It is worth noting that no explicit information about the functions $r(t)$ and $g(t)$ exists. These functions may be directly found only from PA measurements, as well as the amplitude of photoinduced contraction, $v_0$.

Verification of the model in our experiments was done as follows. In the experiment at 3.5°C, the measurements of the PIC contribution dependencies on the laser energy, and the fitting of the experimental waveforms with a signal calculated from expression (5), gave the values of $\phi$, $v_0$ and the function $G(\omega)$. Then, in experiments at $T = 20$–25°C, these values were used to determine $\alpha$ and $R(\omega)$ by the fitting of experimental signals with the two theoretical waveforms calculated from expressions (5),(6). The choice of the relaxation function was facilitated by the obvious time shift between the THE and PIC contributions.

## 3. Results

### 3.1. Measurements at 3.5°C

The experiments were first carried out under dark conditions, and care was taken to avoid any exposure of the sample to light. Each series of measurements started with small values of the laser energies, then the energy was increased stepwise. In an experimental run for each energy level, about 50–70 shots were accumulated. The interval between two runs was 3–5 min (slight variations of the interval did not affect the reproducibility of the measurements). The experiments were repeated several times for different concentrations of RCs, and for the two types of RC. As a first step of the data processing, peak-to-peak amplitude of the PA signal, normalized for the number of RCs, was plotted as a function of the laser energy (expressed as a number of absorbed photons per RC). The results of all our experiments at 3.5°C are combined on the plot in Fig. 5. As follows from Eq. (5), in normalized coordinates the laser energy dependence of the PIC contribution amplitude is fully determined by the parameters $v_0$

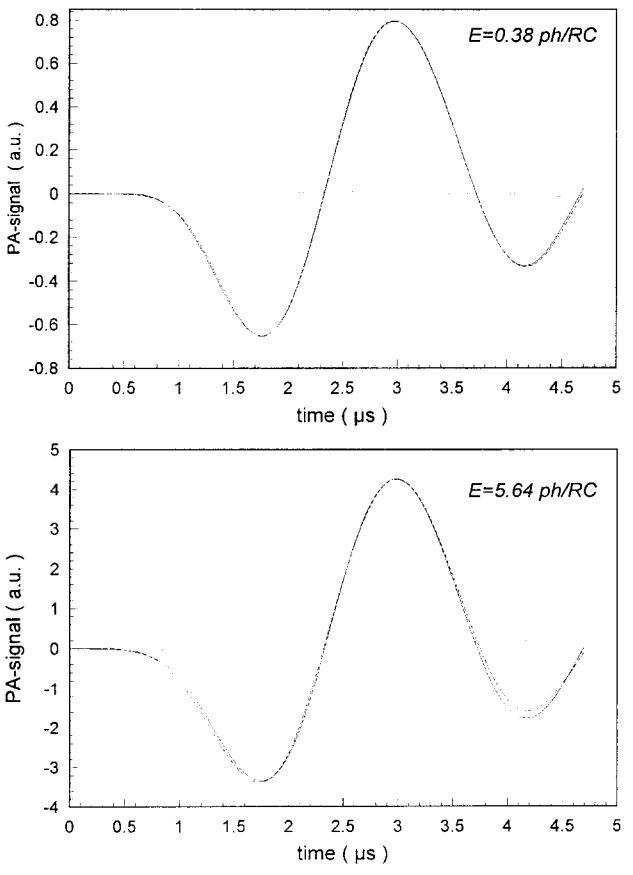


Fig. 6. Theoretical modeling of experimental PA signals observed at 3.5°C at low (A) and high (B) laser energies. Experimental signals are shown by solid lines, theoretical by dashed lines, and residuals by dotted lines.

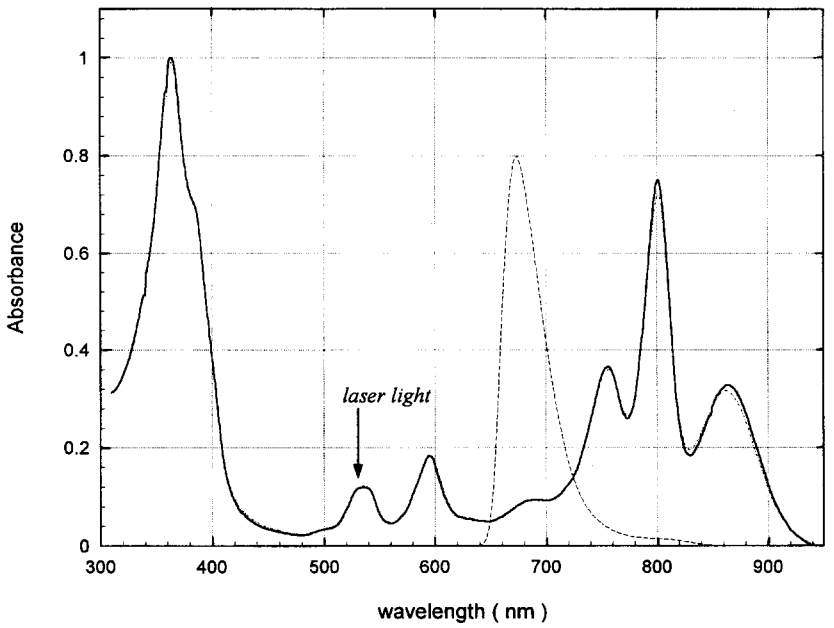


Fig. 7. Absorption spectrum of RCs measured before experiment (solid line), and 10 min after experiment (dashed-dotted line). The spectrum of actinic light is represented by the dashed line.

and $\phi$. The best fit of amplitude data of nine experiments was obtained with a theoretical curve calculated from Eqs. (1) and (5) for $\nu_0 = 32$ Å$^3$ and $\phi = 1$, with the assumption $G(\omega) = 1$. The individual fitting of data points for each experiment and further statistical processing revealed that the statistical accuracy of the measurements was $\pm 1$ Å$^3$. There was no difference between the wild-type and R-26 preparations within the accuracy of our measurements.

In a second step the validity of the theoretical expression (5), and the assumption $G(\omega) = 1$ was checked by the fitting of experimental waveforms for different laser energies. Numerical algorithms were implemented on MATLAB 4.2 software (Math Works). The function LEASTSQ from MATLAB Optimization Toolbox v.1.0c was used for the nonlinear least-square fitting. This function implements two the most popular algorithms: Gauss-Newton and Levenberg-Marquardt. Normally, the first works faster, whereas the second algorithm is more robust. Therefore,

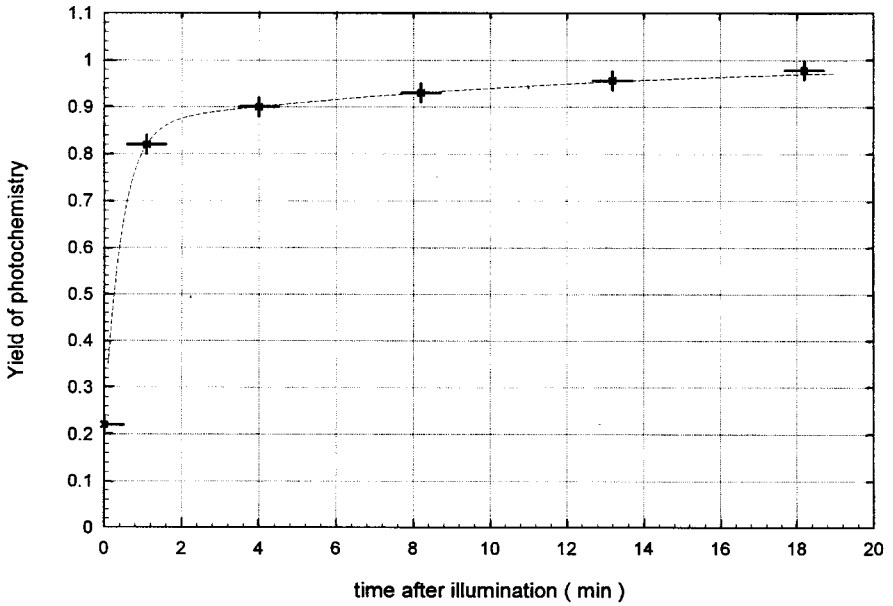


Fig. 8. Recovery of the quantum yield of photochemistry after illumination by the actinic light. The point $t = 0$ corresponds to the measurements under illumination. All the other points are measured under dark conditions.

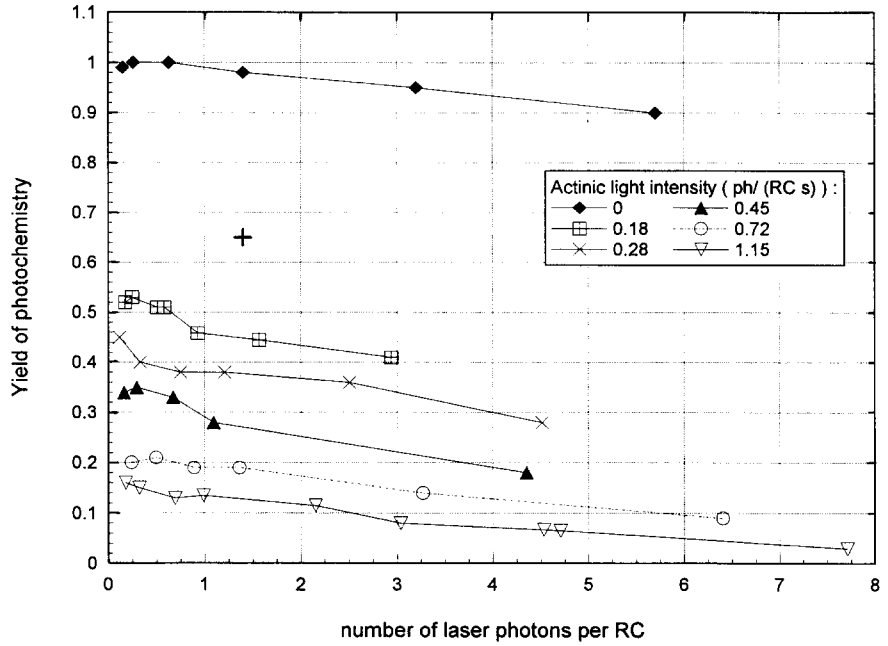


Fig. 9. Dependence of the quantum yield of photochemistry on the laser energy measured at different actinic light intensities. The control measurement in the dark immediately after experiment is shown by the symbol (+).

starting with the Gauss-Newton algorithm, LEASTSQ switches automatically to the Levenberg-Marquardt algorithm when the convergency is poor. As a rule, less than 50 iterations were necessary to arrive at a solution. The results of the fitting are shown in Fig. 6. The good fit of the experimental waveforms for both small and large laser energies means that the photoinduced contraction is rather fast to be resolved by our experimental set-up, justifying that $G(\omega) = 1$. In general, the time resolution of the PA measurements depends on the type of relaxation kinetics function. Thus, in our experimental set-up an arbitrary exponential decay may be resolved from instantaneous decay in the interval of relaxation times 100 ns–5 $\mu$s (see [13] for details). Therefore, the characteristic time of the

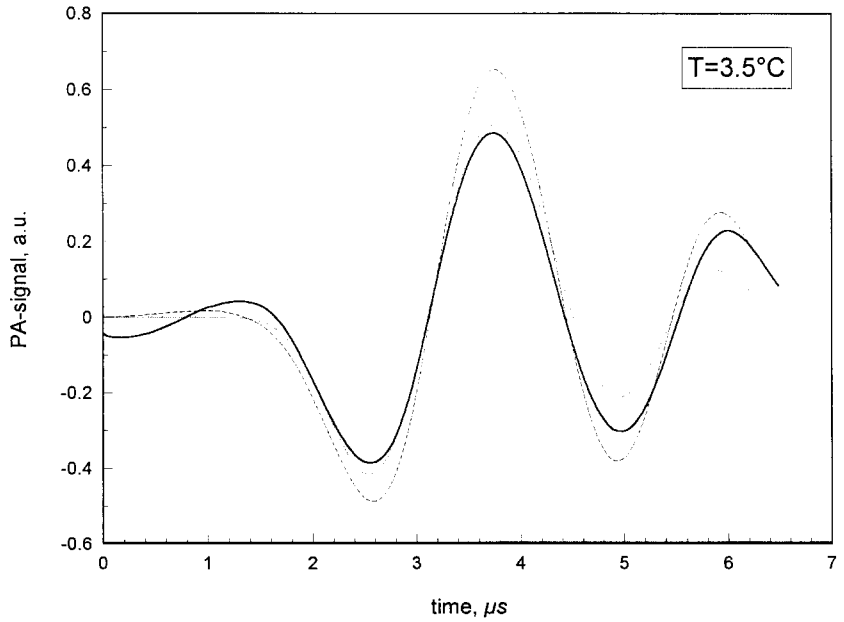


Fig. 10. Anomalous scattering observed at high laser energies under strong actinic light illumination. The solid line represents the PA signal measured at $E = 7$ ph/RC, the dotted line its fit to the model, and the dashed line the PA signal measured at $E = 4.3$ ph/RC.

reverse expansion after the initial contraction must be longer than 5 $\mu$s, which is in agreement with slow time measurements [9].

The measurements of volume changes following the photochemical event turned out to be a very sensitive tool of monitoring the photochemical activity. It was found that in the end of a run of successive measurements at high laser energies the sample displayed less photoactivity. The quantum yield of photochemistry $\phi \approx 1$, found from the fitting of the PA signals at the low laser energies, dropped to 0.9 for energies in the range 100–200 $\mu$J (3–6 photons per RC), and to 0.75–0.85 for energies in the range 200–300 $\mu$J (6–12 photons per RC). The effect was less pronounced with a fresh sample, and the efficiency rose back after some dark adaptation period (5–20 min). To study this effect further we used an additional cw actinic light illumination. The spectrum of the actinic light is shown in Fig. 7, together with the absorption spectrum of RCs. The absorption spectra of the sample were checked before, and 10–15 min after the experiment. The actinic illumination was not strong enough to induce irreversible changes of the sample (the strongest exposure was about $\sim 1$ photon absorbed in a RC per second). The recovery was monitored by the PA measurements of the photoinduced contraction, first in the presence of the actinic light and then in specific times after switching it off. The corresponding changes in the quantum efficiency $\phi$ (found by fitting experimental waveforms with constant $v_0$) is shown in Fig. 8. One can see a two-phase recovery process: one, unresolved, stage takes less than 1 min, and the other approx. 10 min. The experimental points may be closely fitted by two exponentials: $\phi(t) = 1 - C_1 \exp(-t/\tau_1) - C_2 \exp(-t/\tau_2)$. The best-fit curve, shown in Fig. 8 by the dashed line, was calculated with the parameters $C_1 = 0.64$, $\tau_1 = 0.44$ min, and $C_2 = 0.14$, $\tau_2 = 11.9$ min.

Another illustration of the complicated process of the multiphase recovery of the sample is the measurements of $\phi$ as a function of the laser light energy for different actinic light intensities (Fig. 9). The decrease of $\phi$ with the increase of $E$ become more and more pronounced with the elevation of actinic light intensity. The repetition rate of the laser pulses introduces another time scale $\sim 1$ s. For large laser energies ($> 3$ photons per RC) this time is not enough for the full recovery of RC exposed to the actinic light.

It must be noted that the reduction of the PIC contribution in a sample photochemically modified by strong actinic light illumination and irradiated with very high laser energies may not result only from the drop in quantum efficiency. The fitting of the experimental waveforms detected under these conditions was not satisfactory. We also observed strong laser light scattering from the sample under intense illumination. The scattering was seen as a large spurious signal induced in the front surface of the detector by scattered light (Fig. 10). Therefore, the results may be partly attributed to the bleaching of the sample at the laser wavelength (and corresponding increase of elastic scattering), effecting a reduction of the number of photons absorbed by RCs. The bleaching should be more pronounced near the center of the beam and drop at the periphery. This effect causes broadening of the cross-sectional distribution of the PIC, and, thereby, the broadening of the observed signal (see Fig. 10).

To find the changes of $\phi$, corresponding specifically to the effect of the actinic light, the measurements were

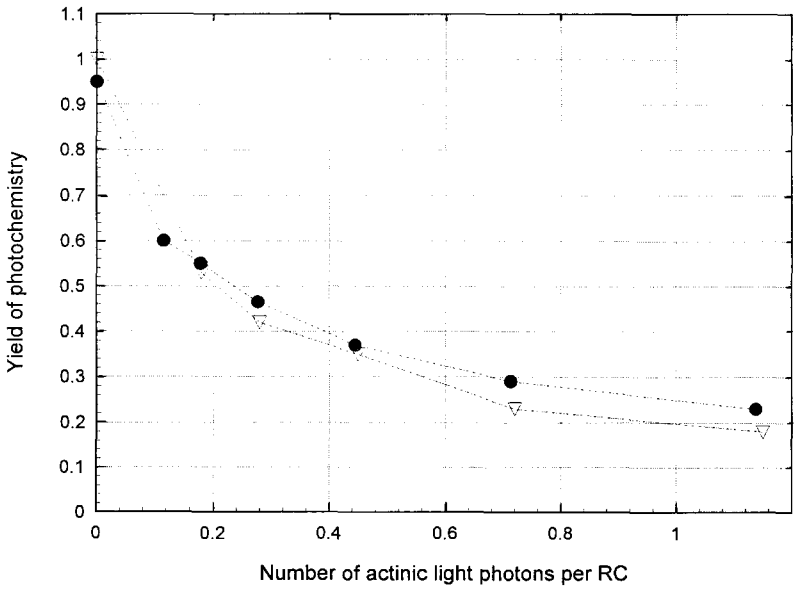


Fig. 11. Quantum yield of photochemistry as a function of the actinic light intensity measured at low laser energy (see comment in the text).

systematically repeated for small, fixed laser energies $E \sim 7\ \mu J$ (0.24 ph/RC) and various actinic light intensities $I$. During the experiment the sample was periodically monitored in the dark, where the quantum efficiency was found to be in the range 0.95–1 throughout the measurements. The results are summarized in Fig. 11.

### 3.2. Measurements at the room temperature

PA measurements were carried out at several temperatures in the range 1–25°C. For an accurate analysis, however, the temperatures 20°C and 25°C were chosen. At these temperatures the changes of the PA signal profile are most pronounced because of the close balance between the two contributions. All room temperature experiments started after control measurements at 3.5°C, which aimed to check the quality of the sample by measuring the parameters $v_0$ and $\phi$ (according to the procedure outlined above). Then, the PIC contribution was calculated from expression (5) (with $G(\omega) = 1$). The THE contribution was obtained by using expression (6). We assumed a two-component exponential relaxation function $r(t) = (A/\tau_a)\exp(-t/\tau_a) + (B/\tau_b)\exp(-t/\tau_b)$. The general fitting scheme comprises seven adjustable parameters: $\alpha$, $\phi$, the relaxation parameters $A$, $\tau_a$, $B$, $\tau_b$, and the time shift between the calculated and measured signals $\Delta$. Nonlinear optimization algorithms become unstable with an increasing number of adjustable parameters, and the results of the fitting are strongly dependent upon the quality of the initial guess. Therefore, it was desirable to cut the number of free parameters. In the first step, to determine the value of the energy storage, $\alpha$, we used the PA signals for laser energies less than one photon per RC. For these energies one can take $\phi = 1$ (this was checked in the control experiments at 3.5°C). In addition, analysis of expression (6) shows that the first term in the brackets vanishes at low energies (all the photons absorbed induce photochemistry), so only two parameters are effective: $\alpha$ and $\Delta$. In series of ten measurements we found that a very good fitting of the experimental waveforms can be obtained with $\alpha = 0.24 \pm 0.02$. A typical fit is shown in Fig. 12A. In all other calculations on the PA signals measured

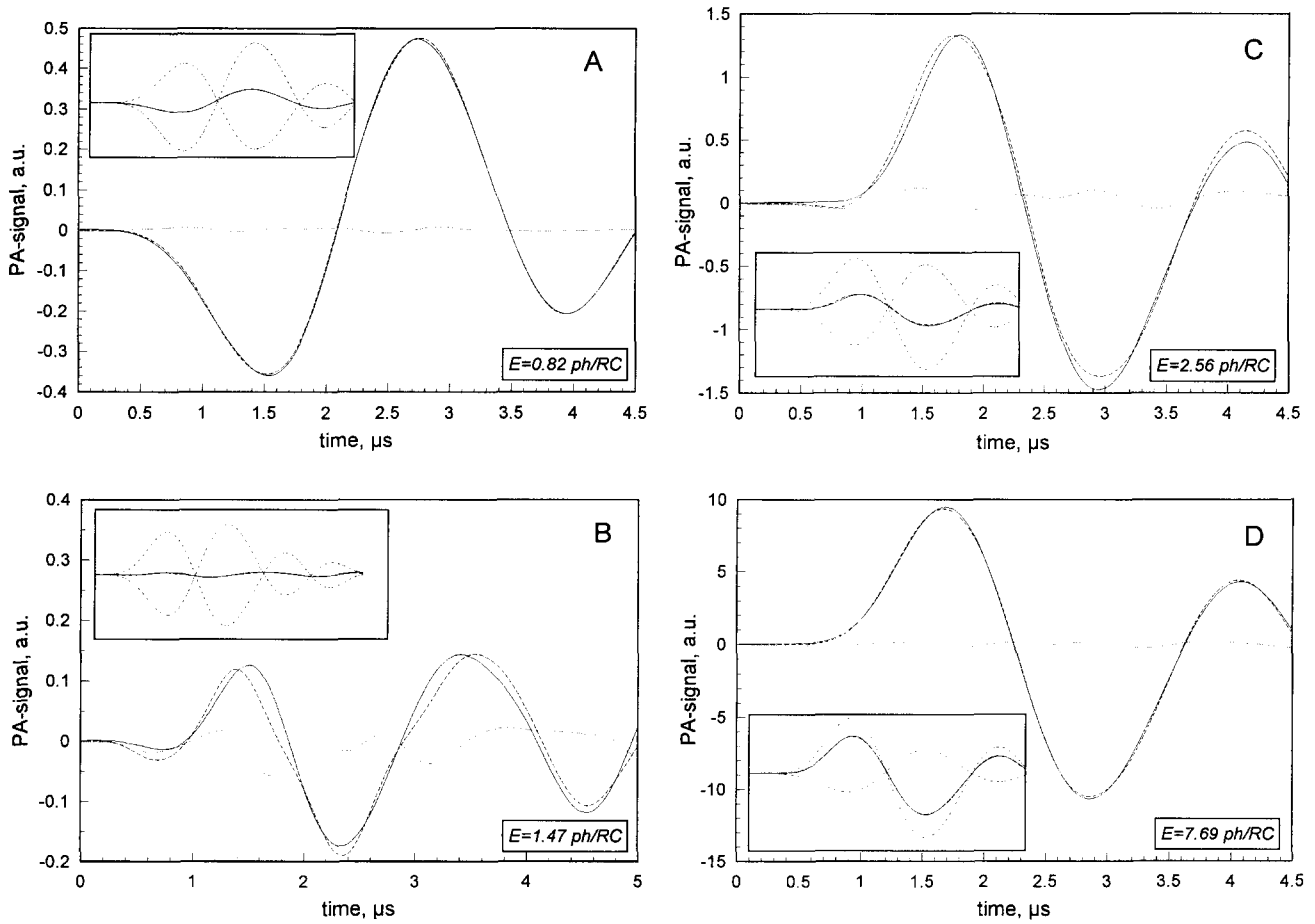


Fig. 12. Experimental PA signals observed at $T = 25$°C at different laser energies, and their theoretical reconstruction with the two-exponential relaxation function. Solid lines represent experimental signals, dashed lines theoretical signals, and dotted lines residuals. In insets are shown the THE contribution (large positive signal), and the PIC contribution (large negative signal) calculated from Eqs. (5) and (6).

at the room temperature we used the same, average parameter $\alpha$. At large laser energies ($E \gg 1$ ph/RC), where

$$V_T(\omega) \approx \frac{\mu\beta}{\rho C_p}\frac{E}{S}D(k)R(\omega) \qquad \text{(cf. Eq. (2))}$$

one can obtain a more reliable estimation of $R(\omega)$. Two particular cases of the general relaxation scheme were considered: (1) one-component decay ($A = 1$, $B = 0$); (2) two-component decay, one instantaneous and the other arbitrary ($\tau_a \to 0$, $A + B = 1$). We found that the two-exponential decay gave a much better fit than one-exponential (Fig. 12C,D). The average value of the best-fit estimations of slow relaxation time constant, found in a number of experiments, is $\tau_b \sim 700$ ns, and the amplitude $B \sim 0.15$. The data obtained indicate the existence of a long-lived intermediate state which is populated when the electron transfer channel is blocked.

The case where the laser energy is about 1 ph/RC is the most complicated for analysis, because the quantum efficiency declines from unity, and the first term in the brackets in Eq. (6), though still small, cannot be neglected. Neither of the two decay processes gave a decisive advantage over the other, and both displayed reasonably good approximation, including all the peculiarities of the very small net PA signals observed at these energies (in Fig. 12B the two-exponential fit is presented).

For a systematic study of the deactivation in a 'closed' RC we used strong actinic light illumination with intensity $I > 1$ ph/(RC s). Taking into account that the relaxation time of $P^+$ is $\sim 1$ s [9,26], we can consider that a steady-state is formed, where almost all RCs are in the charge separated state. In the fitting algorithm we used both one-and two-component models defined above. The result of the calculations are presented in Table 1. The quality of the fit was estimated by $\chi^2$ statistics. The ratio of $\chi^2$ values for the two models, listed in Table 1, shows that the two-component model is a much better approximation. For illustration, a comparison between the typical fits obtained with the two models is presented in Fig. 13. From these results we can deduce that the deactivation process in a 'closed' RC includes some long-lived intermediate state,

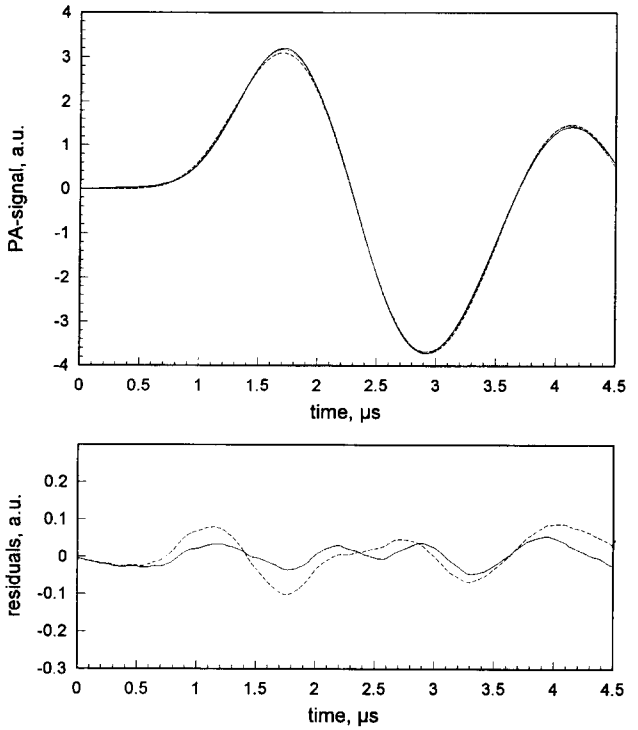


Fig. 13. Theoretical reconstruction of the PA signal observed at strong actinic light illumination conditions ($I = 1.1$ ph/RC per s). Solid line in the upper plot represents experimental waveform, dashed line its theoretical reconstruction with a one component model of the relaxation, and dotted line the reconstruction with the two-component model. In the lower plot the residuals for one-component relaxation are shown by a dashed line, and for two-component model by a solid line. Laser light energy, $E = 2.55$ ph/RC.

corresponding to an exponential decay with a lifetime $\tau_b = 620 \pm 80$ ns and an amplitude $B = 0.14 \pm 0.04$.

An analogous fitting scheme was used to find the yield of photochemistry as a function of the actinic light intensity. The laser energy was chosen $E \sim 7$ μJ (0.24 ph/RC) to avoid a 'double saturation' (by the laser light and the actinic light), and to compare the dependence $\phi(I)$ with the same dependence measured at 3.5°C. The evolution of the PA signal profile with the increase of $I$ at constant $E$ shown in Fig. 14 is quite analogous to that observed for

Table 1
Quantum yield of photochemistry and relaxation times measured at different laser energies under strong actinic light illumination (I = 1.1 ph/(RC s))

| Laser energy $E$ (ph/RC) | One-component decay | | Two-component decay | | | $\frac{\chi^2_2}{\chi^2_1}$ |
|---|---|---|---|---|---|---|
| | $\phi_1$ | $\tau_1$ (ns) | $\phi_2$ | $\tau_2$ (ns) | $B$ | |
| 0.53 | 0.33 | 125 | 0.32 | 580 | 0.08 | 0.75 |
| 1.76 | 0.33 | 189 | 0.31 | 576 | 0.16 | 0.63 |
| 2.55 | 0.33 | 191 | 0.31 | 579 | 0.16 | 0.55 |
| 4.5 | 0.24 | 186 | 0.21 | 533 | 0.18 | 0.68 |
| 5.98 | 0.21 | 159 | 0.18 | 724 | 0.11 | 0.50 |
| 6.94 | 0.21 | 162 | 0.18 | 709 | 0.13 | 0.54 |

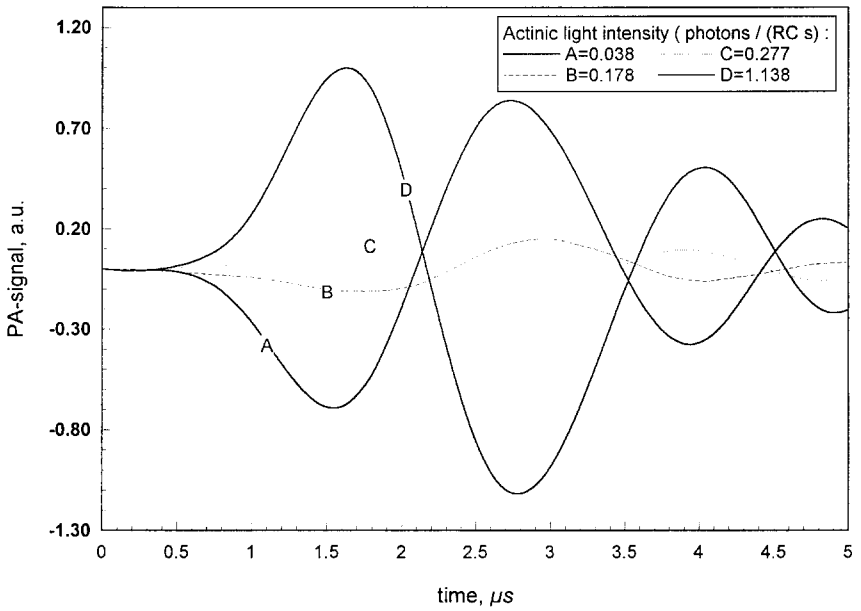


Fig. 14. Transformation of PA signal shape at $T = 25°C$ with the increase of actinic light intensity. Laser light energy, $E \approx 0.24$ ph/RC.

$I = 0$ at elevated laser energies (cf. Figs. 4 and 14). For modeling of the PA signals, a two-exponential decay was assumed. At the small and intermediate intensities (for negative and near zero net PA signals), a variation of relaxation parameters does not affect the quality of the fit, whereas for large energies a good fit was obtained for relaxation parameters $\tau_b$ and $B$ as those listed in Table 1. Nevertheless, it was found that in the whole intensity range even small deviation of $\phi$ from the best-fit value (on $\pm 0.02$) makes the fitting considerably worse for any combination of the relaxation parameters. Therefore, the best-fit values of $\phi$ may be considered as a reliable estimation of the dependence $\phi$ ($I$), which is presented in Fig. 15 in comparison with the analogous dependence measured at 3.5°C (each data point on the plot is an average of few measurements). With normalization to the same value at $I = 0$, both experiments give the same dependence. One can conclude that the temperature dependence of the quantum efficiency is indeed negligible.

## 4. Discussion

Photoacoustic diagnostics is a unique experimental technique providing explicit information about specific volume (or density) changes induced by illumination in a

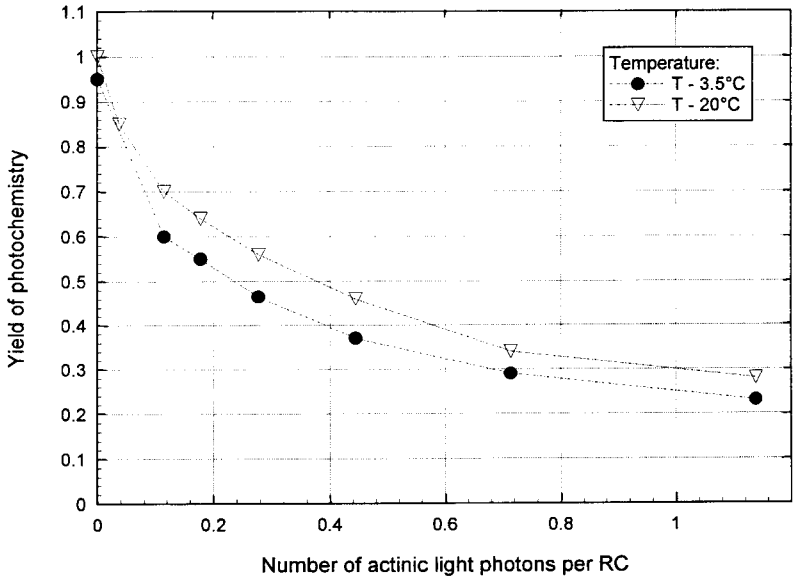


Fig. 15. Quantum yield of photochemistry as a function of the actinic light intensity measured at 3.5°C and 20°C at low laser energy, $E \approx 0.24$ ph/RC.

photochemically active medium. In each particular case, however, one has to discriminate between several possible contributions to the observed volume variations [18]. Photoinduced volume changes in suspension of isolated RCs are combined from the two parts: a contraction, associated with structural changes during the electron transfer and expansion, due to heat released in thermal deactivation processes. These two contributions have different localization in RC-solvent complex. While the photoinduced contraction follows the change in charge distribution across the RC and may be attributed to protein movement, the thermal expansion mainly occurs in the solvent bath in the RC vicinity. This scenario is supported by the fact that the temperature dependence of the thermal contribution in suspension of RCs is the same as in the calorimetric reference. In particular, at 3.5°C, under strong actinic light illumination ($\sim 5-10$ ph/(RC s)), which heavily saturates photochemistry and thereby suppresses the photoinduced contraction, very small net PA signal can be distinguished above the noise level (Fig. 3). Therefore, the thermal contribution vanishes as in the aqueous buffer, which implies a low thermal expansion coefficient for RC proteins. A small thermal expansion of proteins was indeed assumed also in [5]. The effect of zero thermal expansion is unique for dilute aqueous solutions at $\sim 4$°C, and determined by their special structural organization [27], which holds in the vicinity of RC. However, acoustic measurements with standard piezodetectors do not give direct spatial discrimination between the two contributions, and the case of aqueous solutions remains the only one where such separation can be done.

We consider that the photoinduced contraction is directly related to the electron transfer reaction, so in our model the nonlinear dependence on the laser energy of the PIC contribution is explained by the saturation of the laser flash yield (simply, by the fact that the number of the photochemical events is limited by the number of RCs) rather than by a variation of the photoinduced contraction associated with each electron transfer reaction. The absolute value of photoinduced contraction per RC detected in our acoustic experiments on *Rb. sphaeroides* ($32 \pm 1$ Å$^3$) is in a very close agreement with the value $\sim 33$ Å$^3$ (20 ml/mol) found by Arata and Parson in their slow, direct measurements of the volume changes (time resolution $\sim 100$ $\mu$s) [9]. In a previous work by Malkin et al. [10], however, a smaller value (10 Å$^3$) was reported. In that work, the maximum, saturation value of the structural volume changes was not reached and was therefore estimated by extrapolation of the dependence of the volume changes on the laser energy. This procedure could lead to a gross underestimation, and cause the discrepancy. Neither value agrees with recent time-resolved PA measurements [28], where, for the same preparation, a volume change of $\sim 20$ Å$^3$ was found. Fast time resolution of our set-up ($\sim 100$ ns) was still not enough to resolve the dynamics of the initial contraction. One can conclude only that the contraction occurs during the $P^*Q_AQ_B \rightarrow P^+Q_A^-Q_B$ transition, and not in the $P^+Q_A^-Q_B \rightarrow P^+Q_AQ_B^-$ step. This finding is in line with photodichroism measurements of Kirmaier et al. [2], which revealed that bacteriochlorophylls and bacteriopheophytins did not move significantly with respect to each other in the time interval between 2 ns and 10 ms after excitation. In [4] some conformational changes were reported to be associated with a fast (picoseconds) nuclear relaxation within accessory bacteriochlorophyll and/or surrounding protein following the reduction of bacteriopheophytin. In [3,5] the photoinduced contraction is explained by the change in separation and/or relative orientation of the donor-quinone acceptor pair due to electrostatic interactions between $P^+$ and $Q_A^-$, which tends to decrease their separation distance. A possible physiological role of the structural changes is in enhancing charge stabilization [3]. The details of the mechanism and the functional meaning of the changes still have to be clarified.

In the limit of low laser energies, when all photons trapped by the RC induce photochemical reaction, the part of the photon energy (2.34 eV for $\lambda = 532$ nm) released as a heat during initial deexcitation and the $P^*Q_AQ_B \rightarrow P^+Q_A^-Q_B$ reaction was found to be 1.78 eV. Since pressure changes during the photoreaction are negligibly small, the heat release is equal to the enthalpy change, thus the remainder $0.56 \pm 0.04$ eV constitutes the enthalpy of $P^+Q_A^-Q_B$ above the ground state. This value is quite close to the enthalpy change value 0.63 eV for the transition $PQ_AQ_B \rightarrow P^+Q_A^-Q_B$ found from delayed fluorescence measurements in RCs of *Rb. sphaeroides* by Arata and Parson [29], but both estimates are considerably higher than the estimated $\leq 0.13$ eV observed by the same authors in their capacitor microphone experiments [9]. The free energy gap between $P^+Q_A^-Q_B$ and the ground state was previously estimated as $\sim 0.6$ eV [25].

In the absence of an electron donor to $P^+$, only one-electron activity is possible in the RC: $PQ_AQ_B + h\nu \rightarrow P^*Q_AQ_B \rightarrow P^+Q_A^-Q_B \leftrightarrow P^+Q_AQ_B^-$. At high laser energies, as well as under conditions of strong actinic light illumination, when more than one photon is absorbed before reduction of $P^+$, the channel of deactivation of initially excited state through the electron transfer reaction is blocked. The selective excitation with the laser light at 532 nm enables to identify this initial state as an excited state of $Bphe_M$ [25]. The processing of experimental data revealed that in the 'closed' RC the depopulation of this state is well described by two-component decay, a prompt thermalization process (on the time scale of the experiment) and a relatively long lived state, which is characterized by an exponential decay with a lifetime $620 \pm 80$ ns and an amplitude $0.14 \pm 0.04$. The deactivation process in 'closed' RC, which absorbed more than one 'extra' photon, could be quite complicated, however, so these parameters should be considered as an average values for a few different steps. The accuracy of our present deconvo-

lution analysis enabled us to identify only one dominating step in the time window of the measurements (100 ns–5 $\mu$s).

Measurements of photoinduced structural changes by the PA method are a precise tool to monitor photochemical activity, as has been already pointed out in Ref. [14]. The dynamics of $P^+$ dark relaxation in *Rb. sphaeroides* RCs at neutral pH goes via electron transfer from $Q_B^-$ back to $Q_A$ and then to $P^+$, and takes $\sim$ 1 s [26]. This explains the fast recovery stage after long actinic light illumination, which was not resolved in our measurements. However, full recovery of pigment/protein complex takes a few minutes as shown in Fig. 8. The slow recovery stage is likely to be explained by existence of long term light-induced changes in the pigment/protein structure, which affect the normal contraction-expansion cycle.

The time resolution of our present set-up ($\sim$ 100 ns) is not enough to resolve the dynamics of the photoinduced contraction following the electron transfer reaction, and fast thermal deactivation processes. We hope to increase substantially (up to 1 ns) the resolution with a new PA cell which was built to implement potentials of the front face irradiation scheme described in [13,30]. Experiments in this direction are now underway in our laboratory.

## Acknowledgements

This work was supported in part by the Basic Research Foundation of the Israel Academy of Sciences and Humanities and by the Willstatter Center for Photosynthesis. The work of O.V.P. was supported by postdoctoral fellowship of the Feinberg graduate school of the Weizmann Institute of Science. We thank P. Gast and A. Hoff from the Biophysics Dept., State University of Leiden, The Netherlands, for the reaction center preparations. We acknowledge the kind support of A. Scherz and technical assistance of V. Brumfeld.

## References

[1] Zinth, W. and Kaiser, W. (1993) in The Photosynthetic Reaction Center (J. Deisenhofer and J.R. Norris, eds.), Academic Press, pp. 71–88.
[2] Kirmaier, G., Holten, D. and Parson, W.W. (1983) Biochim. Biophys. Acta 725, 190–202.
[3] Kleinfeld, D., Okamura, M.Y. and Feher, G. (1984) Biochemistry 23, 578–5786.
[4] Tiede, D.M., Kellogg, E. and Breton, J. (1987) Biochim. Biophys. Acta 892, 294–302.
[5] Hoganson, C.W., Windsor M.W., Farkas D.I. and Parson W.W. (1987) Biochim. Biophys. Acta 892, 275–283.
[6] Braslavsky, S.E. and Heihoff, K. (1989) Photothermal Methods, in: CRC Handbook of Organic Photochemistry (J.C. Scaiano, ed.), Vol. 1, CRC Press, Boca Raton, pp. 327–356.
[7] Peters, K.S. and Snyder, G.J. (1988) Science 241, 1053–1057.
[8] Callis, J.B., Parson, W.W. and M. Gouterman (1972) Biochim. Biophys. Acta 267, 348–362.
[9] Arata, H. and Parson, W.W. (1981) Biochim. Biophys. Acta 636, 70–81.
[10] Malkin, S., Churio, M.S., Shochat, S. and Braslavsky, S.E. (1994) J. Photochem. Photobiol. B: Biol. 23, 79–95.
[11] Hermann, M.S. and Goodman, J.L. (1989) J. Am. Chem. Soc. 111, 1849–1854.
[12] Egerev, S.V., Lyamshev, L.M. and Puchenkov, O.V. (1990) Sov. Phys. Usp. 33, 739–762.
[13] Puchenkov, O.V. (1995) Biophys. Chem. (in press).
[14] Delosme, R., Bèal, D. and Joliot, P. (1994) Biochim. Biophys. Acta 1185, 56–64.
[15] Okamura, M.Y., Debus, R.J., Kleinfeld, D. and Feher, G. (1982) in Function of Quinones in Energy Conserving Systems (Trumpower, B.L. ed.), pp. 299–317, Academic Press, New York.
[16] Weast, R.C. (ed.) (1980) CRC Handbook of Chemistry and Physics, CRC Press, Boca Raton.
[17] Puchenkov, O.V. (1994) J. Physique IV, Coll. C7, 225–228.
[18] Patel, C.K.N. and Tam, A.C. (1981) Rev. Mod. Phys. 53, 517–550.
[19] Malkin, S. Lasser-Ross, N., Bults, G. and Cahen, D. (1981) in Structure and Molecular Organization of the Photosynthetic Apparatus (Akoyunoglou G., ed.), pp. 1031–1042, Balaban, Philadelphia.
[20] Kaye, G.W.C. and Laby T.H. (1973) Tables of Physical and Chemical Constants, Longman.
[21] Braslavsky, S.E. and G.E. Heibel (1992) Chem. Rev. 92, 1381–1410.
[22] Rudzki-Small, J., Libertiny, L.J. and Small, E.W. (1992) Biophys. Chem. 42, 29–37.
[23] Malkin, S. (1974) Biophys. Chem. 2, 327–337.
[24] Straley, S.C., Parson, W.W., Mauzerall, D.C. and Clayton, R.K. (1973) Biochim. Biophys. Acta 305, 597–609.
[25] Kirmaier, C. and Holten, D. (1993) in The Photosynthetic Reaction Center (Deisenhofer, J. and Norris, J.R., eds.), pp. 49–70.
[26] Shinkarev, V.P. and Wraight, C.A. (1993) in The Photosynthetic Reaction Center (Deisenhofer, J. and Norris, J.R., eds.), pp. 193–255.
[27] Kunz, W., Bellisent-Funel, M.-C. and Calmettes, P. (1989) in Treatise on Bioelectrochemistry, Vol. I., pp. 5–67.
[28] Mauzerall, D.C., Gunner, M.R., and Zhang, J.W. (1995) Biophys. J. 68, 275–280.
[29] Arata, H. and Parson, W.W. (1981) Biochim. Biophys. Acta 638, 201–209.
[30] Arnaut, L.G., Caldwell, R.A. Elbert, J.E. and Melton, L.A. (1992) Rev. Sci. Instrum. 63, 5381–5389.